Case Studies in Thermal Engineering 49 (2023) 103298

Contents lists available at ScienceDirect

Case Studies in Thermal Engineering

journal homepage: www.elsevier.com/locate/csite

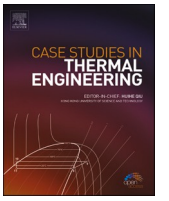

Experimental studies on sidewall pool fire for assessing green façades hazard

Xianjia Huang [a], Jinkai Wang [b], He Zhu [b], Chaoliang Xing [a], Tharindu Lakruwan Wickremanayake Karunaratne [c], Cheuk Lun Chow [c,*], Wan Ki Chow [d]

[a] Joint Laboratory of Nuclear Power Plant Fire Safety, Guangzhou Institute of Industrial Technology, Guangzhou, 511458, China
[b] State Key Laboratory of Nuclear Power Monitoring Technology and Equipment China Nuclear Power Design Co., Ltd., Shenzhen, 518045, China
[c] Department of Architecture and Civil Engineering, City University of Hong Kong, Hong Kong, China
[d] Department of Building Environment and Energy Engineering, The Hong Kong Polytechnic University, Hong Kong, China

ARTICLE INFO

Handling Editor: Huihe Qiu

Keywords:
Average flame height
Sidewall
Rectangular fire source
Mirror model

ABSTRACT

Fire hazard assessment on green façade used to be carried out by a window plume. Large amount of fuel was burnt. A small pool fire placed adjacent to the façade can give similar effect on assessing the hazardous consequences. Fire plume characteristics provide important information of fire hazards adjacent to façade. The average flame height of rectangular source fire located against different sidewall materials were investigated in this study.

Burning tests were conducted with rectangular burners of different dimensions with adjacent walls of different thermal properties, including steel plate and calcium silicate board. Experimental results of fire source with sidewall were compared with those in open space. Due to sidewall blockage, a deep necking-in structure was observed at the flame base and entrained air for combustion. Effect of aspect ratio of the fire pool and effect of heat loss through a sidewall on the average flame height were investigated. Convection lost would decrease the temperature of the fuel-air mixture and should not be ignored. On average, the mean flame height of the fire source with steel plate was 1.08 times that with calcium silicate board. A model for estimating the average flame height was developed by modifying the mirror model.

Nomenclature

C_p	Specific heat capacity of air (J/kg •K)
D	Diameter of burner (m)
D^*	Characteristic diameter of axis-symmetric burner, Eq. (2)
D^*_w	Characteristic diameter of rectangular burner, Eq. (10)
EF	Entrainment factor
g	Acceleration due to gravity, (m/s^2)
L	Length of rectangular burner, (m)
L_f	Average flame height, (m)

* Corresponding author.
E-mail address: cheuchow@cityu.edu.hk (C.L. Chow).

https://doi.org/10.1016/j.csite.2023.103298
Received 13 March 2023; Received in revised form 5 July 2023; Accepted 14 July 2023
Available online 15 July 2023

P^*	Effective perimeter, (m)
$\dot{Q}$	Fire heat release rate, (kW)
$\dot{Q}_D^*$	Dimensionless heat release rate for axis-symmetric fire, Eq. (3)
$\dot{Q}_{wp}^*$	Dimensionless heat release rate for rectangular burner, Eq. (5)
$\dot{Q}_s^*$	Dimensionless heat release rate for rectangular burner, Eq. (6)
RN	Aspect ratio
s	Area of burner (m^2)
T	Temperature of sidewall, (K)
T_∞	Ambient temperature, (K)
W	Width of rectangular burner, (m)
Greek symbols	
ρ_∞	Ambient air density, (kg/m^3)

1. Introduction

There are special façades in tall green buildings including vertical greenery systems (VGS) [1], photovoltaic (PV) panels [2] and water wall system (WWS) [3] designed to satisfy the criteria for green and sustainable buildings. There are no prescriptive fire codes on such green constructions yet [4]. Fire hazards of special façades arise from window plume of post-flashover room fires [5] as in Fig. 1. However, a large quantity of fuel is required to keep a developed room fire in experiments to create window plumes. Similar effect of a window plume can be studied by a smaller pool fire placed next to the special facade as in Fig. 1 as reported by Refs. [6,7]. This is particularly useful in assessing fire hazards of green buildings with special facades [1,2].

The average flame height is an important parameter to study the fire response of an object. Flame height is used to predict the thermal radiation flux of flame [8,9].); estimate the fire power with inverse modeling [10]; contact area of flame with sidewall and analysis the thermal flux from flame to the sidewall [11]. When a rectangular fire source is located near a wall, the heat would be lost from the flame to the sidewall through radiation and convection [12,13]. In addition, air entrainment to the flame is reduced tremendously due to the obstruction of the sidewall. The sidewall effect on a rectangular pool fire characteristics has to be studied properly as reported by Ref. [9].

[14] developed two simple models to estimate the flame height generated from wall-attached fire source. The average flame height L_f is given by the entrainment factor EF and the heat release rate $\dot{Q}$:

$$L_f/D = 0.132\frac{\dot{Q}^{2/5}}{EF^{2/3}D} \tag{1}$$

As the model did not include the effect of aspect ratio, an equation was proposed later by Ref. [15]:

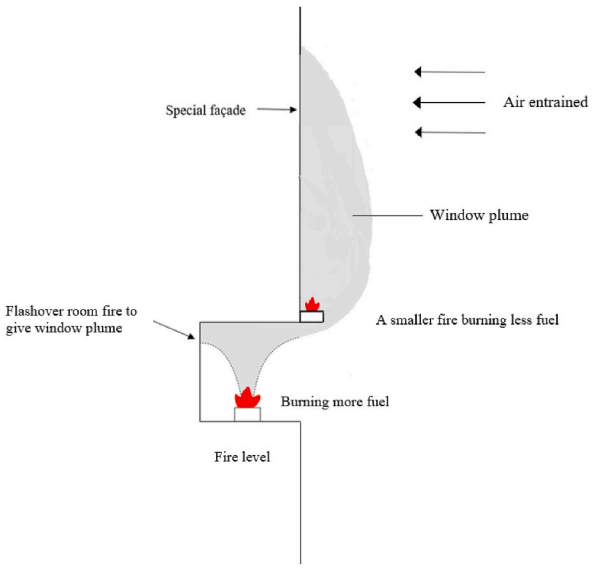

Fig. 1. Smaller fire at wall.

$$\frac{L_f}{P^*} = \begin{cases} 3.89\dot{Q}_{wp}^{*\,2/5} & \dot{Q}_{wp}^{*} > 0.3 \quad (a) \\ 5.47\dot{Q}_{wp}^{*\,2/3} & \dot{Q}_{wp}^{*} \le 0.3 \quad (b) \end{cases} \tag{2}$$

where

$$\dot{Q}_{wp}^{*} = \frac{2\dot{Q}}{\rho_\infty c_p T_\infty g^{1/2} (P^*)^{5/2}} \tag{3}$$

where P^* is given by Ref. [15]:

$$P^* = 2(L + 2W) \tag{4}$$

Most of these earlier studies such as the mirror model by Ref. [16] assumed the sidewall to be adiabatic without heat lost [17]. Effect of heat loss through the sidewall in applying the mirror model will be focused on in this paper. The flame height of pool fire was studied for a sidewall with high thermal conductivity (steel), and low thermal conductivity (calcium silicate, CS). This is different from previous works [9,18], which assumed an adiabatic sidewall. The average flame height was estimated with heat loss from the flame taken into account. Then, the correlation for estimating the mean flame height of rectangular fire burners against a steel plate was investigated.

2. Experimental details

The experimental setup in this study is shown schematically in Fig. 2. The surface area of the rectangular burner was all 900 cm^2 as reported before [19]; 2021b). The CS sidewall was of length 2.44 m, width 1.22 m, thickness 0.008 m, with density 925 kg/m^3, conductivity 0.15 W/m • K, and specific heat capacity 1.0 kJ/kg • K. The steel sidewall was of length 1.5 m, width 1 m, thickness 0.0003 m, with density 7860 kg/m^3, conductivity 68.4 W/m • K, and specific heat capacity 0.46 kJ/kg • K. The fire scenarios are presented in Table 1, two tests on each.

Two digital CCD camera operating at 25 frames/s were used to record the flame shape. The average flame height was taken to be the transient value of 50% intermittency [19] in this study. Flames recorded for a steel sidewall ($\dot{Q}$ = 84.8 kW) is shown in Fig. 3a. Several sub-flames can be observed for an aspect ratio above 7.45. This is consistent with the observation in Refs. [8,19].

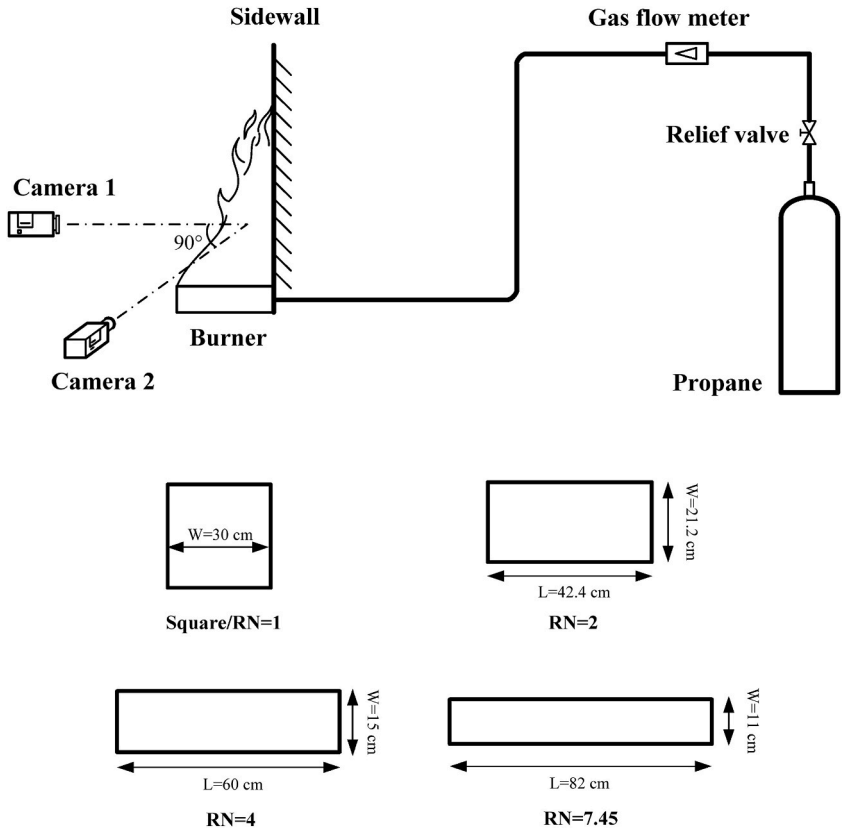

Fig. 2. Burner against a sidewall of different materials [9,19].

Table 1
Summary of tested fire scenarios.

Burner shape	Surface area (cm^2)	Burner		Aspect ratio *RN*	Fire power $\dot{Q}$ (kW)
		Length (cm)	Width (cm)		
Square	900	30.0	30.0	1	28.3; 42.4; 56.5; 70.7; 84.8
Rectangular	900	42.4	21.2	2	
Rectangular	900	60.0	15.0	4	
Rectangular	900	82.0	11.0	7.4	

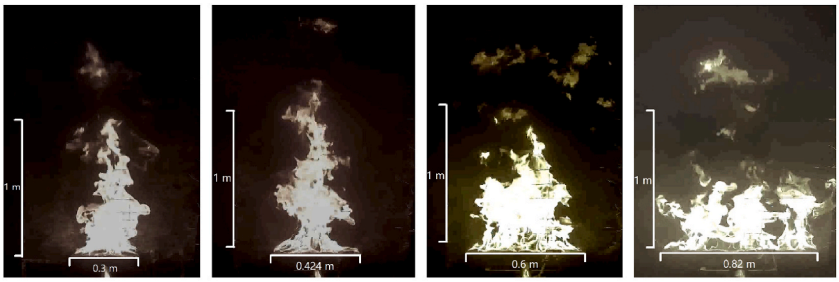

Fig. 3. Flame morphology of fire source against a steel plate ($\dot{Q}$ = 84.8 kW).

3. Experimental results

3.1. Sidewall effect on flame morphology

Flame image for the rectangular fire located against the steel plate and the CS board, at time intervals of 0.08 s (RN = 7.45 and $\dot{Q}$ = **84.8 kW**) are shown in Fig. 4a and b respectively. The sidewall blocked a significant portion of the entrained air. To entrain sufficient air for fuel combustion, a deep necking-in structure was created at the base of flame.

As a comparison, sequential flame images for the pool fire in the open space are shown in Fig. 5, at intervals of 0.08 s (RN = 7.45 and $\dot{Q}$ = 84.8 kW). As the fire experiments using rectangular burner were conducted in the open space, small flamelet vortices were generated at the base of flame, as indicated by the yellow arrows in Fig. 5. Air was entrained into the fuel from both sides of the rectangular burner. Compared with fire source against a sidewall, more air was entrained into the flame and the flame height was considerable shorter.

3.2. Sidewall effect on flame height

Fig. 6 shows the average flame height for rectangular burner in the open space and located against a sidewall made of different materials. The sidewall effect on the average flame height is significant. For the rectangular burner in the open space and without a sidewall constraint, the average flame height decreased as shown in Fig. 6a. As the rectangular burner was located against a sidewall, the average flame height reached a maximum value at an aspect ratio of 2 for the CS board, and at an aspect ratio of 4 for the steel plate, as shown in Fig. 6b.

For a rectangular burner located against a CS sidewall and placed in the open space, the effective perimeter (Eq. (4)) was inversely related to the average flame height. When the rectangular burner was placed in the open space, its effective perimeter increased from 2.4 m to 3.72 m with the aspect ratio shown by the blue dotted lines in Fig. 6a. As the aspect ratio increased, the decreased average flame height was 0.18 m in average, and its average reduction rate was 23.8%. For the burner located against a CS board, the effective perimeter of the rectangular burner with an aspect ratio of 2 was 1.696 m, which was the minimum value. Air entrainment rate was the

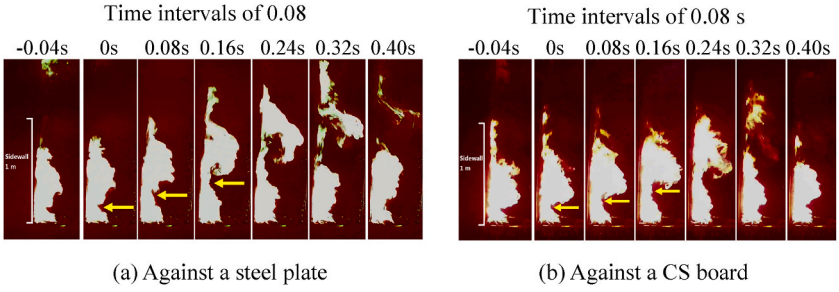

Fig. 4. Flame morphology during pulsation for fire source against sidewall (RN = 7.45, $\dot{Q}$ = 84.8 kW).

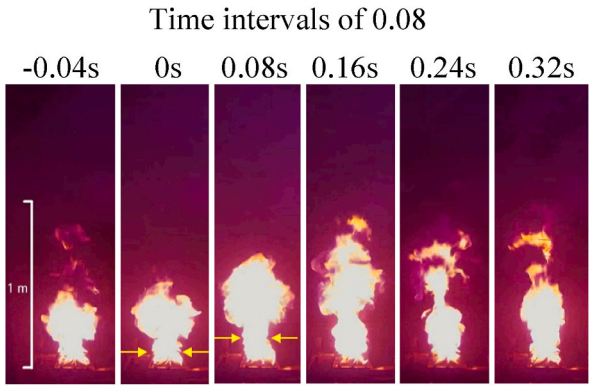

Fig. 5. Flame morphology during pulsation for fire source in open space (RN = 7.45, $\dot{Q}$ = 84.8 kW).

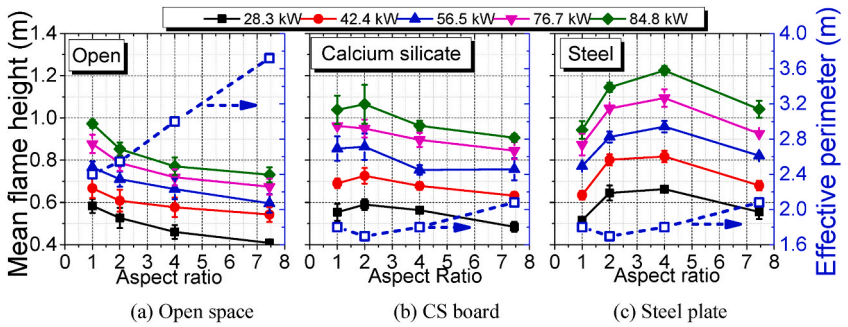

Fig. 6. Average flame height for rectangular burner in the open space and located against a sidewall made of different materials.

smallest at the base of the fire in all four tests, which led to a maximum average value. Evidently, the average flame height decreased as the effective perimeter of the rectangular burner increased.

For the rectangular burner located against a steel plate, there was a higher heat transfer between the flame and the upper part of the steel plate, which influenced the average flame height. The average flame height increased as the aspect ratio increased from 1 to 4 and decreased from 4 to 7.45, as shown in Fig. 6c. Compared with a burner located against a CS board, the thermal convection between the steel plate and the flame led to more heat loss of the flame. This heat loss decreased the temperature of the air-fuel mixture. Therefore, the fuel-air mixture required additional time to complete the reaction to achieve efficient combustion. This led to a higher average flame height from the rectangular burner with a steel plate, as compared to that of the burner against a CS board. A higher the heat loss from the steel plate led to a decrease in the flame temperature. The flame height was observed to increase as compared to that of the

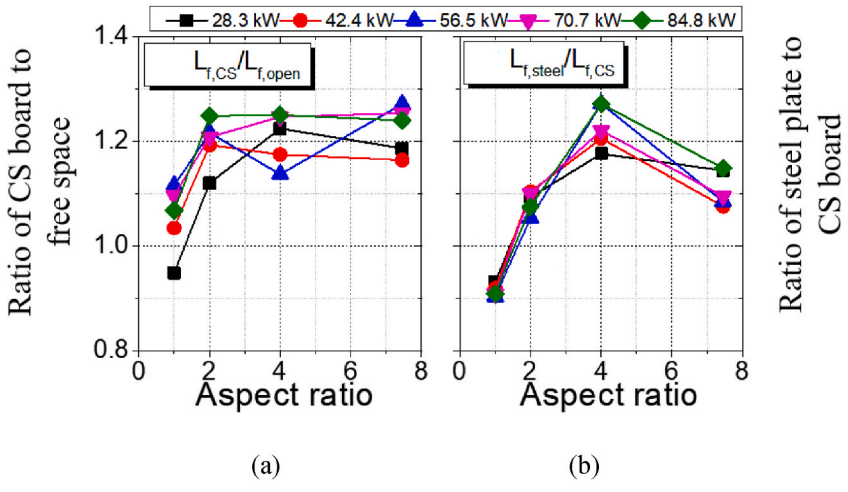

Fig. 7. Ratios of the average flame heights under different conditions.

rectangular burner against a CS board.

Increase in aspect ratio had two opposing effects on the mean flame length of rectangular burner:

- The interaction area between the flame and steel increased, and heat loss from the flame to the surrounding air increased. This lowered the air-fuel mixture temperature. The mixture thus required a longer time and greater distance for burning. Hence, the average flame height increased.
- The air entrainment rate increased, leading to more complete combustion at a lower height and thus the average flame height decreased.

The combined action of these two opposing effects resulted in a maximum average flame height at an aspect ratio of 4 (Fig. 6c). As the aspect ratio increased from 1 to 4, the average flame height increased. However, the average flame height decreased as the aspect ratio changed from 4 to 7.45. Evidently, the heat loss effect dominated for aspect ratio from 1 to 4 and the air entrainment effect dominated for aspect ratio from 4 to 7.5.

Fig. 7 presents ratios of the average flame heights under different conditions. The ratio of the average flame height of the burner with the CS board to that of the burner in the open space was approximately 1.17 in the case of the rectangular burner with an aspect ratio exceeding 1, as in Fig. 7a. The effect of the aspect ratio was insignificant as reported by Ref. [15]. For the burner placed against the steel plate of high thermal conductivity, the relative instantaneous flame height increased by less than 1.27 comparing to CS plate of low thermal conductivity, the average relative increase was 1.08, as in Fig. 7b.

4. Average flame height model

4.1. CS board sidewall

Fig. 8 compares the prediction made using Eq. (2) with this study and those available in the literature [12,14,15,17,20,21]. Generally, the experimental data and data from the literature, for the sidewall made of low conductivity materials, Eq. (2) has good estimation of the average flame height (Hasemi 1980/81). The experimental data for the average flame height in the present study conform to Eq. (2b). Evidently, this experimental setup was proved appropriate for investigating the sidewall effect on the flame height.

4.2. Steel plate sidewall

The relative increase of average flame height due to the steel plate can be considered as a constant based on the analysis above. Compared with the average flame height of the burner with the CS board, the relative increase of the average flame height is around 1.08 for the burner placed against the steel plate. Based on Eq. (2b), the model of the average flame height of the rectangular burners with steel sidewalls can be expressed as

$$\frac{L_f}{P^*} = 5.9\dot{Q}_{wp}^{*\,2/3}\ \dot{Q}_{wp}^{*} \le 0.3 \tag{5}$$

Fig. 9 compares the prediction obtained using the average flame height model for a fire source against a steel plate in this study and literature copper plate results [13,15]. The prediction error was approximately 15%, which indicates a good accuracy of model prediction.

5. Conclusions

This paper has focused on the effect of sidewall material on the average flame height of rectangular fire sources for assessing fire hazard of green facades. Fire experiments using rectangular burner were performed against steel plate (high thermal conductivity, CS board (low thermal conductivity) and in the open space.

The heat loss from flame to the steel plate was higher than that to the CS board. This heat loss decreased the temperature of the air-fuel mixture. Therefore, the fuel-air mixture required additional time to complete the reaction to achieve efficient combustion. This led to a higher average flame height of the rectangular burner with a steel plate, as compared to that of the fire source with a CS board. The relative increase of average flame height of the rectangular burner with the steel plate is the most prominent for rectangular burner with an aspect ratio of 4.

The mirror model can be modified for estimating the average flame height of a fire source against a steel plate with small thickness. The relative increase of the average flame height generated by the fire source with a steel plate can be considered as a constant value, as compared to that generated by the fire source against a CS board. Based on a comparison of the prediction obtained using the modified model with this study and literature, the prediction error of this modified approach was within 15%.

In summary, research content in this paper is that a series of fire tests were carried out with sidewall and without sidewall. A total of 60 fire tests were conducted excluding repeated fire experiments. Furthermore, a model for estimating the average flame height was developed for fire source located against the materials with high thermal conductivity such as steel plate.

Funding

The work described in this paper is jointly supported by the International Science and Technology Cooperation Project of Guangdong Province China (2022A0505050026); the Research Grants Council of the Hong Kong Special Administrative Region, China for the project “A Study of Energy Harvesting and Fire Hazards Associated with Double-Skin Green Façades of Tall Green Buildings”

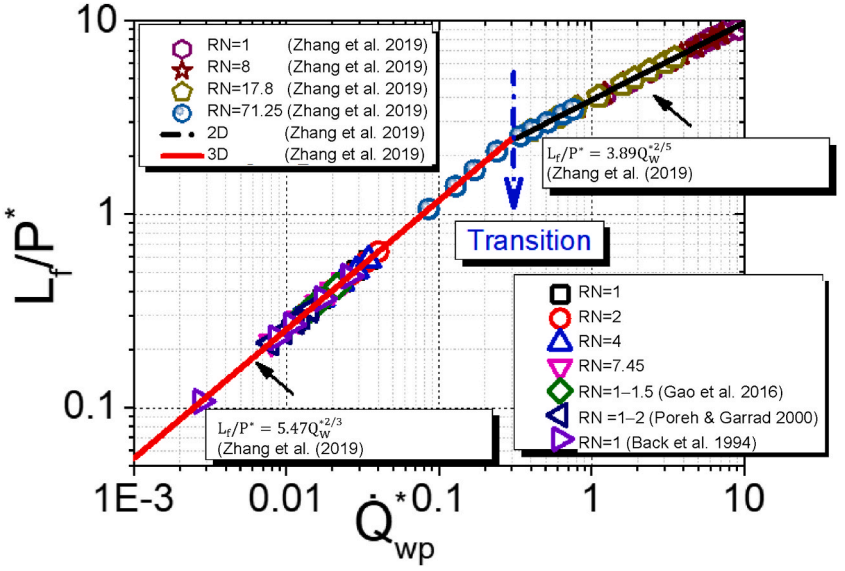

Fig. 8. Comparison the prediction made using Eq. (2) with this study and those available in the literature.

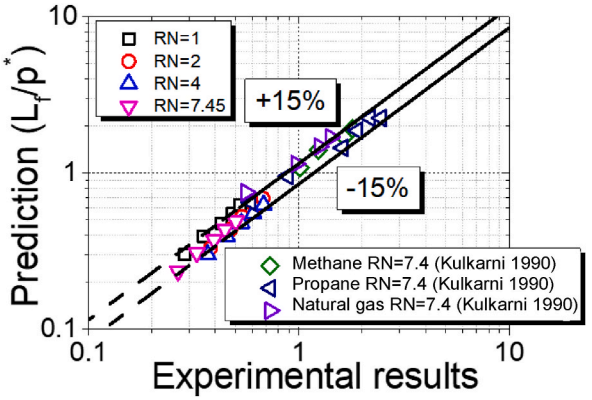

Fig. 9. Comparison of predictions of developed model with experimental data.

(Project No. R1018-22F) and the City University of Hong Kong Strategic Research Grant for the project "Improving the use of positive pressure ventilators to fight enclosure fires" (Project No. 7005662).

Author contributions

Xianjia HUANG: Conceptualization, Methodology, Formal Analysis, Investigation, Writing—original draft preparation, Project administration, Funding acquisition. Jinkai WANG: Conceptualization, Methodology, Formal Analysis, Resources. He ZHU: Conceptualization, Investigation, Resources. Chaoliang XING: Investigation, Validation, Data curation. Tharindu Lakruwan Wickremanayake KARUNARATNE: Validation. Cheuk Lun CHOW: Validation, Funding Acquisition. Wan Ki CHOW: Writing—review and editing, Supervision.

Declaration of competing interest

The authors declare that they have no known competing financial interests or personal relationships that could have appeared to influence the work reported in this paper.

Data availability

No data was used for the research described in the article.

References

[1] C.L. Chow, W.K. Chow, Full-scale Burning on Vertical Greenery system." 2019 Engineering Mechanics Institute Conference, Mini-Symposium on "Emerging Topics and New Developments in Structural Fire Engineering", 18-21 June 2019, Caltech, Pasadena, CA, 2019.
[2] C.L. Chow, S.S. Han, X.M. Ni, A study on fire behaviour of combustible components of two commonly used photovoltaic panels, Fire Mater. 41 (2017) 65–83.
[3] T. Wu, C. Lei, A review of research and development on water wall for building applications, Energy Build. 112 (2016) 198–208.
[4] W.K. Chow, Performance-based approach to determining fire safety provisions for buildings in the Asia-Oceania regions, Build. Environ. 91 (2015) 127–137.
[5] C.L. Chow, Numerical studies on smoke spread in the cavity of a double-skin façade, J. Civ. Eng. Manag. 17 (3) (2011) 371–392.
[6] L. Miao, C.L. Chow, A study on window plume from a room fire to the cavity of a double-skin façade, Appl. Therm. Eng. 129 (2018) 230–241.
[7] L. Miao, C.L. Chow, Influence of heat release rate and wall heat-blocking effect on the thermal plume ejected from compartment fire, Appl. Therm. Eng. 139 (2018) 585–597.
[8] X.J. Huang, X.J. Zhuo, T. Huang, et al., Thermal radiation model for the buoyancy-controlled diffusion plumes from rectangular fire sources, Int. J. Therm. Sci. 150 (2020), 106234.
[9] X. Huang, Y. Wang, H. Zhu, et al., Experimental study on the radiant heat flux of wall-attached fire plume generated by rectangular sources, Int. J. Therm. Sci. 159 (2021), 106605.
[10] K.Y. Li, S.H. Mao, R. Feng, Estimation of heat release rate and fuel type of circular pool fires using inverse modeling based on image recognition technique, Fire Technol. 55 (2019) 667–687.
[11] C.L. Xing, X.J. Huang, J.K. Wang, et al., Heat transfer from the wall-attached flame to the sidewall composed of different materials, Int. J. Therm. Sci. 184 (2023), 107918.
[12] G. Back, C. Beyler, P. Dinenno, Wall incident heat flux distributions resulting from an adjacent fire, Fire Saf. Sci. 4 (1994) 241–252.
[13] A.K. Kulkarni, Radiative and total heat feedback from flames to surface in vertical wall fires, Exp. Heat Tran. 3 (1990) 411–426.
[14] M. Poreh, G. Garrad, A study of wall and corner fire plumes, Fire Saf. J. 34 (2000) 81–98.
[15] X.L. Zhang, L.H. Hu, M.A. Delichatsios, et al., Experimental study on flame morphologic characteristics of wall attached non-premixed buoyancy driven turbulent flames, Appl. Energy 254 (2019), 113672.
[16] E.E. Zukoski, T. Kubota, B. Cetegen, Entrainment in fire plumes, Fire Saf. J. 3 (3) (1980) 107–121.
[17] Y. Hasemi, T. Tokunaga, Some experimental aspects of turbulent diffusion flames and buoyant plumes from fire sources against a wall and in a corner of walls, Combust. Sci. Technol. 40 (1984) 1–17.
[18] X.J. Huang, J.K. Wang, H. Zhu, et al., Flame-splitting mechanism of buoyancy-controlled diffusion plumes generated by a rectangular fire source attached to sidewall, Int. J. Therm. Sci. 179 (2022), 107670.
[19] X.J. Huang, X.J. Zhuo, T. Huang, et al., Simple flame height correlation for buoyancy-controlled diffusion plumes generated by rectangular sources fire with different aspect ratios, Fuel 254 (2019), 115655.
[20] Z.H. Gao, J. Ji, C.G. Fan, et al., Experimental analysis of the influence of accumulated upper hot layer on the maximum ceiling gas temperature by a modified virtual source origin concept, Int. J. Heat Mass Tran. 84 (2015) 262–270.
[21] Z.H. Gao, Z.X. Liu, J. Ji, et al., Experimental study of tunnel sidewall effect on flame characteristics and air entrainment factor of methanol pool fires, Appl. Therm. Eng. 102 (2016) 1314–1319.